Global optimization of smart lightweight structures

R. Salloum[1], O. Heuss[1], D. Mayer[1]
[1] Fraunhofer Institute for Structural Durability and System Reliability LBF,
Bartningstraße 47, 64289 Darmstadt, Germany
e-mail: **rogerio.salloum@lbf.fraunhofer.de**

Abstract
Modern vehicles are constrained to lower CO2 emissions and therefore to have reduced mass compared to ancient designs. In order to accomplish that, the replacement of metals by lightweight composite materials is an interesting option, but this can significantly change the NVH behavior of the vehicle, thus requiring new design techniques. In this context, much research has been done in the last decades to understand the so-called shunted systems, which consist of electromechanical transducers, like piezoelectric ceramic transducers, applied to a mechanical structure and connected to an electronic shunt circuit, so as to reduce structural vibrations. Consequently, lightweight design can be combined with the advantages of shunted systems, which can significantly improve NVH characteristics without excessive mass addition. As a promising area of research, this paper presents a methodology for a global design of a smart structure, instead of isolated sub-systems, where different functions of the electromechanical system (host structure, transducers and electronics) are simultaneously optimized. This paper concentrates on numerical investigations of composite materials and focus on semi-active vibration control. In order to show the effectiveness of this method, an initial composite part is improved by shape optimization, regarding its mass, durability, static and dynamic behavior. During this phase, the effective (or generalized) electromechanical coupling coefficient (EMCC), which describes the energy transfer between the mechanical and the electrical systems, is also optimized. Finally, an optimized shunt circuit is connected to the system, showing that high vibration attenuation and high mass gain can be both attained.

1 Introduction

Since the 1990s, there has been an enormous growth in smart structures technology. Several fields of study benefit from this development, such as space vehicles, aircrafts, railway and automotive systems, robots, heavy machinery, medical equipment, etc. A wide range of applications include noise and vibration suppression, damping increase, structural health monitoring, energy harvesting, etc. A smart structure typically consists of a host structure, actuators and sensors, a microprocessor that analyzes the signals, a control law to change the characteristics of the structure and integrated power electronics. More importantly, a smart structure has the ability to adapt its properties according to external stimuli in a controlled manner. Several types of structures, actuators, sensors and control laws have been studied and published. Potential applications for smart structures are presented in [1].

In this paper, investigations are targeted at composite materials. In the context of smart structures design, they are often a reasonable choice, since they present a good stiffness to weight ratio. Fiber-reinforced composites allow more possibilities than commonly used materials and their custom-designed nature offers a unique opportunity to minimize weight, embed actuators and improve dynamic behavior.

The main problems that appear when designing a lightweight structure, however, can be related to high vibration levels, due to low mass and damping inherent to composite materials. In order to attenuate this undesirable effect, passive methods can be used, e.g. mechanical tuned mass absorbers (TMD), but they are often associated with a high mass added onto the structure. Active vibration control, on the other side, can effectively reduce vibrations, but there is always the need for actuation power and relatively high demand for computational controller performance.

Between these two techniques are situated the semi-passive and the semi-active methods, which benefit from low cost components and a simple controller design. These techniques consist of applying a piezoceramic to a mechanical structure and then connecting it to a shunt circuit. In that way, it is possible to change the mechanical properties of the complete system without the need of actively driving the actuator. Various types of shunts have already been developed and tested regarding their potentials and characteristics in vibration control. However, they are not yet integrated in many technical structures, due to the high effort to design a semi-active device, since there are many correlated parameters that have to be optimized in order to get an applicable solution.

In this context, it has already been evidenced in the literature [2] that optimizing an actuator on pre-determined host structures, and vice versa, is little effective. More importantly, when considering shunting techniques, the EMCC is the driving parameter, so its optimization is necessary. A number of analytical or numerical methods for optimizing smart structures have been published [3] [4] [5], but metals and academic geometries are usually used, only active control is considered and no experimental data is used in the design loop whatsoever. The work presented in this paper is initially interested in numerical results as design guidelines. Nevertheless, the notion of considering measured data throughout the optimization process is already introduced.

In order to show that shunting techniques can be applied to technical structures, attention will be given to one very important component in a passenger vehicle: the control arm, commonly named wishbone. It is part of the widely used MacPherson suspension and connects each front wheel to the subframe or directly to the chassis. It usually has a flat triangular shape that pivots in two vertices, whereas one end is connected to the steering knuckle at the wheel, allowing the vertical movement of spring and damper. Other than assuring maneuverability of the vehicle and holding the wheel during brake or acceleration, the wishbone is one of the main transfer paths for vibrations coming from the wheels into the chassis. The reduction of these vibrations is often a design objective that is related to the comfort of passengers, for example when driving through a rough roadway or running over small obstacles. Vibrations from the road can be partly isolated by rubber bushings in the two pivots, but in order to achieve better noise and vibration performance, changes in other vehicle parts might be necessary. These include the application of absorbing foam materials on the chassis or vibration absorbers in the powertrain, which have a high cost in mass and eventually in fuel consumption.

So as to avoid these correction measures, the goal of this research is to develop a smart wishbone, especially designed with lightweight materials, capable of absorbing vibrations through a piezoceramic and a shunt circuit. The right-hand wishbone used for this study is shown in Fig. 1.

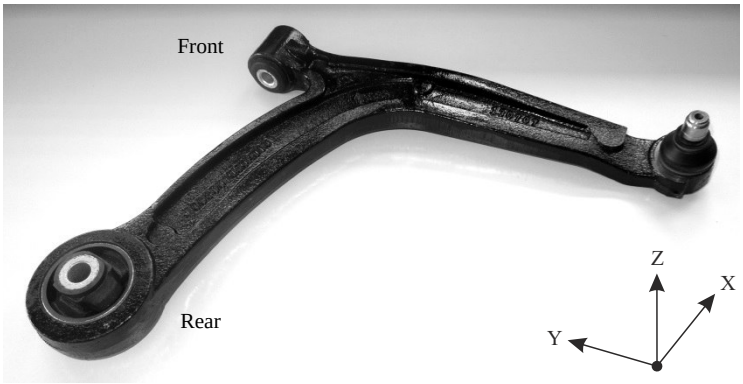

Figure 1: The wishbone

This study is divided in five sections. Section 2 describes how to benefit from the original metal wishbone and design a composite structure with similar characteristics. Section 3 then points out the key challenges in including a piezoceramic in a composite structure. Section 4 presents a possible semi-active shunting technique and what design challenges there are. Section 5 puts together the three domains, showing how the optimization is carried out. Finally, section 6 presents the numerical results and shows how the simultaneous approach can be advantageous.

2 Lightweight Design

2.1 Metal Structure Simplification

In order to efficiently design the lightweight composite structure, a set of technical specifications regarding mass, boundary conditions, static and dynamic variables must be defined. In the case of replacing metal structures by lightweight solutions, an evaluation of the pre-existing metal part allows the creation of an initial design that can be later optimized and eventually meet these specifications.

During the concept phase, technical specifications are usually defined based on knowledge of previous systems or on numerical analysis. Early-stage experimental identification of prototypes can be very costly and time consuming. In this way, physical tests are often carried out in later development phases, in order to update numerical predictions. Therefore, the characteristics of a commercially available (Fiat 500) steel wishbone have been numerically analyzed. By using realistic excitation levels, it is possible to simulate its static and dynamic behavior, so as to evaluate the possibility of applying semi-active vibration control on complex-shaped structures.

A preliminary finite element (FE) study was carried out using a CAD model built from the approximate dimensions of the part. Since the elastic characteristics of the rubber bushings play a major role in the overall behavior, their static stiffness was obtained from the manufacturer. In the FE model, the two bushings of the wishbone were connected to an ideally rigid subframe. The right end was rigidly connected to a mass, which correspond to the wheel and the steering knuckle together. It was also connected to a linear spring, which represents the vertical and the horizontal suspension of the wheel.

In order to reduce the large number of variables to be analyzed, some assumptions are made. No rotational degrees of freedom (DOF) or transverse efforts (Y direction) will be taken into account, since most part of the dynamic efforts inputted at the wheel occurs in the X-Z plane. When passing over a small obstacle, for example, the wheel first suffers an impact contrary to the direction of travel (X direction) and then rolls over the obstacle (Z direction). In some cases, however, efforts in the Y direction can be higher than in the X-Z direction, depending on the suspension design, tire characteristics, road roughness, frequency range, etc.

First, a static analysis was carried out to calculate the stiffness of the component when it is subjected to longitudinal (brake and acceleration) or vertical efforts. In the first case, a static force of 16,9 kN was applied at the right end of the wishbone in the X direction, and in the second, 10,5 kN in the Z direction. The resultant stiffness were equal to 4,00 and 0,35 kN/mm, respectively.

Then, a modal analysis allowed the identification of important eigenfrequencies that could contribute to the noise and vibration performance of the vehicle. The first eight eigenfrequencies included in the range 0-250 Hz are represented in Table 1. In this frequency range, it is important to keep vibration levels as low as possible, since any superposition between modes of the wishbone and other vehicle components (subframe, suspension, tire, etc.) could increase noise and therefore deteriorate comfort.

Mode	Freq. (Hz)	Dyn. strain (10^{-5})	Mode	Freq. (Hz)	Dyn. strain (10^{-5})
1	11,3	0,6	**5**	80,3	1,3
2	15,6	18,3	**6**	111,1	1,8
3	48,6	6,7	**7**	127,9	1,8
4	58,4	14,9	**8**	204,3	4,3

Table 1: Calculated wishbone eigenfrequencies and respective maximum dynamic strains

Finally and most importantly, a harmonic analysis of the steel wishbone has been carried out. This analysis aims at the vibration transmission through the wishbone, i.e. how much of the input forces at the wheel pass through the bushings into the subframe. The inputs are hence defined as translational forces at the right end, whereas outputs are reaction forces across the front and rear bushings. These transfer functions are called transmissibility. For each direction of force input, it shows how much amplification (or reduction) there is in each direction in each bushing. Fig. 2 shows some simulated transmissibility transfer functions of the wishbone.

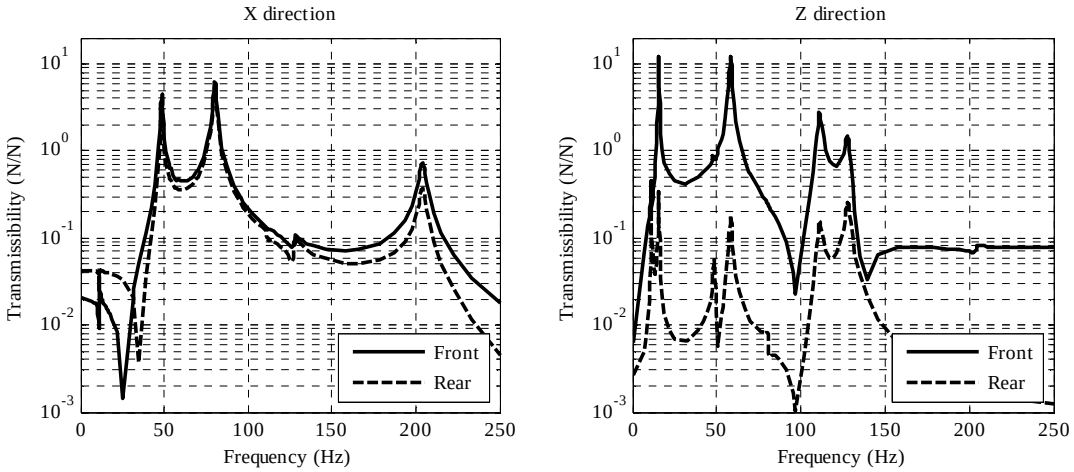

Figure 2: Transmissibility of the wishbone in two orthogonal directions

The transmissibility allows the identification of transmission paths, which is important to analyze dynamic stress and strain distribution for each eigenfrequency. It is important to keep in mind that this distribution may differ from the static case. From the point of view of a smart structure, when integrating a piezoceramic to perform vibration control, for example, the dynamic case should be considered.

Following the transmissibility analysis, the highest peaks are investigated, using a constant force of 20 N over the entire frequency range. This assumption, however, may not always represent the real spectrum of input efforts at the wheel. In reality, the dynamic strain for the 8th mode could be for example higher than for the 3rd mode, as the real efforts could be higher at around 200 Hz than at 50 Hz.

This approach allows the identification of two different behaviors at a given eigenfrequency: dynamic and rigid body. In the dynamic behavior, the strain level inside the material is considerably high, so a piezoceramic can be efficiently integrated. In the rigid body behavior, the motion is supported by the bushings, so the strain is low. Therefore, from the shunting technique perspective, a piezoceramic would have little or no effect, since the EMCC might be potentially low.

To reduce vibrations related to the rigid body behavior, it is advisable to have suitable rubber stiffness, damping and proper bushing orientation, since radial and axial directions have different properties. On the other hand, dynamic behaviors can be theoretically influenced by shunting techniques.

In a first approach, only two eigenfrequencies will be chosen. This will allow an easier understanding of physical phenomena by studying a simplified structure, e.g. a beam, instead of complex geometries. Once the techniques are well comprehended, they can be applied in a more complex design.

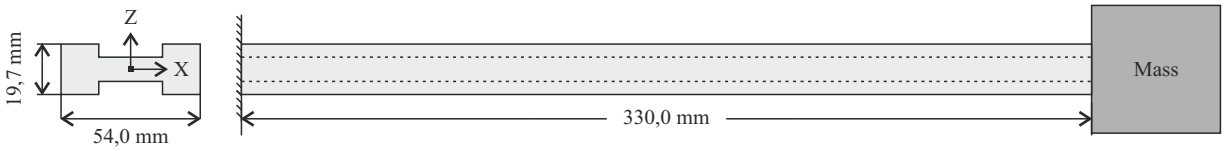

Figure 3: Simplified metal beam (I-beam)

A mode shape analysis of the wishbone revealed that the 2nd and 4th modes have a predominant vertical movement (Z direction), whereas the 3rd and the 8th have a horizontal movement (X direction). Considering two orthogonal modes, distant enough from each other and inside the audible range, the 4th and 8th modes have been chosen for the following analyses. Next, a simplified structure with similar static and dynamic behavior is designed. It consists of an I-beam with a constant cross-section, as depicted in Fig. 3, representing the approximate dimensions of one part of the wishbone. One end of the beam is ideally clamped and a mass is attached to the other. A shape fit has been carried out to adapt the beam's behavior to the wishbone's. The applied efforts have also been adapted, in order to match stress and strain levels and facilitate experimental analysis in the future.

Property	Wishbone		Simplified metal beam	
Structural mass (kg)	5,26		2,11	
Tip mass (kg)	22,50		1,57	
	Z direction	**X direction**	**Z direction**	**X direction**
Static force (kN)	10,5	16,9	0,2	0,2
Static stiffness (kN/mm)	0,35	4,00	0,35	3,98
Eigenfrequency (Hz)	58,4	204,3	59,6	202,5
Dynamic force (N)	20,0	20,0	3,33	3,33
Max. dyn. stress (MPa)	29,3	8,5	35,0	10,0
Max. dyn. strain (10^{-5})	14,9	4,3	13,9	4,0

Table 2: Wishbone and simplified structure characteristics

The numerical results are summarized in Table 2. In the subsequent sections, the characteristics of the simplified metal beam will be used as specifications for the composite part and the development of the lightweight smart structure.

2.2 Composite Part Modeling

Once the characteristics of the metal structure are set, it is desirable to have a composite part with the same passive performance, but suitable for the application of a piezoceramic and a shunt circuit. In that sense, an FE model of the composite structure was built using ANSYS Composite PrepPost software. It is based on the classical laminate theory and facilitates the analysis of layered composite structures using numerous variables. Composites provide stiff and lightweight design, with enough flexibility for complex shapes, but it often requires high efforts to define input variables in an optimization. In this sense, the engineering of a composite product is an iterative process. This involves stress and deformation evaluation and, in the case of an insufficient design or material failure, the geometry or laminate has to be modified and the evaluation is repeated.

For this reason, when optimizing a composite part, a compromise must be found between several input and output variables, since a mathematical global optimum might be difficult to attain. Among the input variables there is the part geometry, the fiber material (carbon or glass), the type of layer (unidirectional or woven), the thickness and number of layers, layup sequence, ply orientation, etc. Output variables include mass, resultant static stiffness, stress and strain levels, failure criteria, etc. Moreover, the manufacturing process should be kept in mind during the design process, in order to keep production complexity and costs low. In the case of a smart structure, where an actuator will be included afterwards, it is also important to analyze the position of the piezoceramic in advance in order to improve strain levels and to optimize the EMCC.

2.3 Failure Criteria

In composites design there is a strong need for simple failure criteria that are physically representative. A well-established and commonly used criterion is the one developed by Puck [6]. It considers two distinctive types of failure, fiber and inter-fiber, which model the brittle behavior of composites, and additionally three different fracture modes.

ANSYS Composite PrepPost includes the Puck failure criteria calculation, provided the material constants are known. The final criterion can be represented through the reserve factor, which is the factor all existing stresses would have to be multiplied with, in order to originate failure. Throughout the optimization process, the reserve factor is defined among the output variables and it is hence assured that a minimum value of one is attained. This factor evaluates the permissible static load that can be applied on a composite part before it fails. Despite the fact that the real excitation on a smart structure is dynamic, it is possible to identify weak spots in the structure. This can lead to a better overall design, potentially reducing weight by redistributing layers or by correctly positioning the piezoceramic.

3 Piezoceramic Transducer

The term piezoelectricity refers to the effect present in many natural crystals that is the generation of electricity under mechanical pressure. It was first observed by the Curie brothers in 1880 but had no practical application until the First World War, when it was used in ultrasonic emitters. With the discovery of piezoceramics exhibiting better piezo effect than natural materials, like the lead zirconate titanates (PZT), a large scale manufacturing became possible and the application in adaptive structures grew.

In the last decades, piezoceramics became the major type of actuator being investigated for smart structures. Much research has been done trying to efficiently put together metal structures and surface-bonded actuators, but few technical applications can be found where piezoceramic materials and composite structures are designed together. Still several considerations have to be taken into account when designing such systems, for example the EMCC, the load carrying capability, durability, manufacturing techniques, etc.

3.1 Modeling

The piezoelectric effect can be expressed in terms of a linear constitutive equation (Eq. 1) that is derived from basic thermodynamic relations. Here, ε represents the strain vector, σ, the stress vector, D, the vector of electric displacement, E, the vector of applied electric field, **S**, the compliance matrix, **d**, the matrix of piezoelectric strain constants and $\mathbf{e}^{\sigma}$, the permittivity matrix at constant stress.

$$\begin{bmatrix} \varepsilon \\ D \end{bmatrix} = \begin{bmatrix} S & d^{T} \\ d & e^{\sigma} \end{bmatrix} \begin{bmatrix} \sigma \\ E \end{bmatrix} \tag{1}$$

In the FE model, the linear constitutive equation is embedded in a piezoelectric 20-node solid element. The material characteristics for the piezoceramic PIC151 (compliance, piezoelectric strain and permittivity matrices) are provided by the manufacturer. This permits an analysis of mechanical and electrical DOF in order to define input and output variables during the optimization process.

3.2 Durability Considerations

A piezoceramic has no moving parts and its displacement is based on solid state dynamics, it shows hence almost no wear, a fact that makes it suitable for dynamic applications. There is, however, no generic formula to determine its lifetime, but parameters like temperature, humidity, voltage, acceleration, frequency, load, insulation, etc. have an influence on its durability.

Most failures with piezoceramics occur because of excessive mechanical stress. The ceramic material is brittle and cannot withstand high tensile or shear forces. As mentioned in [1], most existing works investigate the effect of compressive loads on piezoceramics. Compressive stresses tend to align the polarization direction perpendicular to the direction of stress, which can destroy some of the initial polarization in a permanent way. On the other hand, limited work has been done considering tensile loads, but published data indicate that the static tensile strength of a typical piezoceramic is around 90 MPa.

According to [7], PZT ceramics can withstand pressures of up to 250 MPa without breaking, but depolarization already occurs at 20% from that limit. Tensile loads of non-preloaded piezoceramics are limited to between 12 and 25 MPa, which are conservative values that will allow long lifetime for the transducers. In this paper, throughout the optimization process, this threshold is defined among the output variables and will be therefore not exceeded.

From the composite design perspective, other than introducing an active function into the structure, the piezoceramic might have other impacts. If it is inserted within a material with different properties, it can induce crack propagation and facilitate delamination. Inversely, when correctly designed, it can act as a protector, holding fibers together thus protecting the material and potentially increasing durability.

4 Semi-Active Shunt Damping

Semi-passive and semi-active techniques take advantage of electromechanical transducers, like piezoceramics, which are capable of converting mechanical energy into electrical energy and vice versa. In a structure incorporating a piezoceramic, its stiffness acts in parallel with the stiffness of the host structure. Hence, by connecting it to a shunt circuit, as represented in Fig. 4, its mechanical impedance can be controlled and the dynamic response can be improved. In the context of this paper, the shunting technique will be used to increase damping in the structure, hence the shunt damping term.

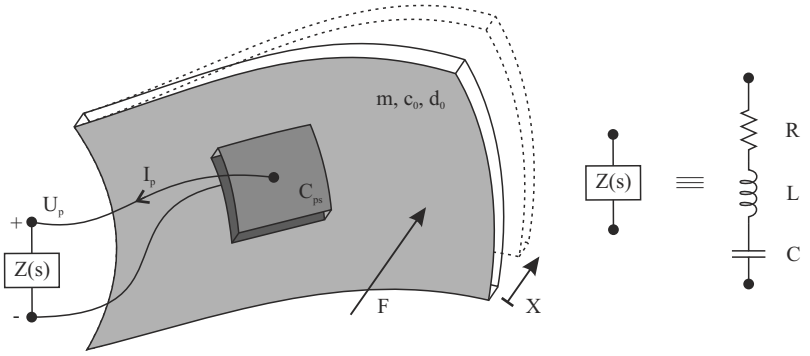

Figure 4: Principle of an RLC-shunt applied to a mechanical structure

The most basic electric circuit to reduce vibrations with a shunted system is the purely passive resistive shunt (R-shunt). It has been introduced in [8], where the analytical equations for the electromechanical system have been derived.

Additionally, [8] introduced the resistive resonant shunt (RL-shunt), in which an inductor is connected to the piezoceramic and the resistor. Since the piezoceramic electrically behaves as a capacitor, the resultant RLC circuit is a damped resonant system, which can be tuned to a certain frequency (e.g. the eigenfrequency of the mechanical system) and can therefore perform similarly to a mechanical TMD. This technique can be better applied on structures with a clear resonant vibration, since it has narrowband effectiveness. With respect to technical applications, the needed inductance value can be very high, maybe tens or hundreds of Henry. For that reason, a synthetic impedance has to be used, a gyrator circuit, which inverts the impedance of a passive element present in the circuit. Here, no power for actuation or signal processing is needed, but since the circuit needs a power supply, this technique is defined as semi-passive. The optimal resistance and inductance values, for which the electrical energy dissipation is maximized, and therefore the mechanical displacement is minimized, have been derived. It is also stated that the optimal values highly depend on the EMCC.

4.1 RLC-shunt Circuit

A method of artificially increasing the EMCC and therefore partly getting rid of its dependency has been investigated in [9]. It is suggested that the use of a negative capacitance, together with an RL-shunt, highly improves vibration attenuation, a fact that has been shown both analytically and experimentally. When a series negative capacitance is connected to a mechanical system, it behaves as a spring element with a negative stiffness, thus reducing its eigenfrequency. Moreover, if a negative capacitance is inserted into an RL-shunt, the two arising poles, characteristic for the absorption effect of the RL-shunt, spread away from each other, making this application efficient in a broader frequency range. Another advantage is that the needed optimal inductance value is much smaller compared to the value of a pure RL-shunt. It can be therefore enough to use a physical coil instead of a gyrator, which can simplify circuit design.

In this study, focus will be given to the RLC-shunt, in which a resistor, an inductor and an additional capacitor are connected to the piezoceramic. At last, the shunt using a negative capacitance is defined as

semi-active, since it transmits external energy in form of actuation forces to the host structure, still without the need of sensor information.

4.2 Negative Impedance Converter

Since there is no passive element with a negative capacitance value, one possible technique for obtaining such an element is to use a synthetic impedance. The circuit shown in Fig. 5 belongs to a general class of circuits known as negative impedance converter (NIC) and has been first applied by [10] in the context of shunt damping. This relatively simple circuit is based on an operational amplifier (op-amp) and performs a signal inversion of a passive element, in this case, a capacitor.

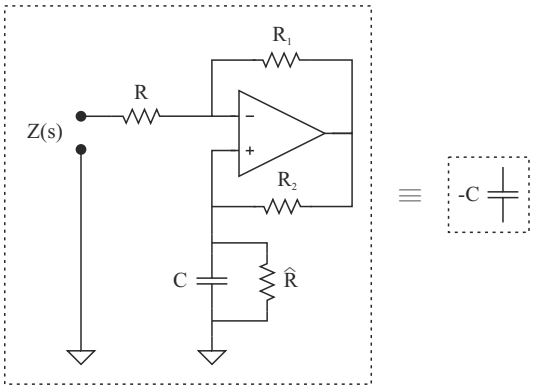

Figure 5: Negative impedance converter (NIC)

Considering an ideal op-amp, it can be assumed that the impedance at the terminals is described by Eq. 2, when a limited frequency band is considered. A more detailed analysis could also consider this electronic circuit as a closed-loop controller, where the effects of feedback (in this case, positive and negative) and of the op-amp parameters must be well understood in order obtain the right impedance transfer function.

$$Z(s) \cong -\frac{R_1}{R_2}\frac{1}{Cs} \tag{2}$$

4.3 Stability

As mentioned before, a negative capacitance can significantly improve the performance of an RL-shunt. However, if not tuned correctly, it can destabilize the system. The main advantage of the RLC-shunt compared to the RL-shunt is that the maximum attenuation depends very little on the EMCC. Nevertheless, the disadvantage of a small EMCC is that the optimum negative capacitance value will be very close to the stability boundary.

As derived by [11], the electromechanical system connected to a negative capacitance has a stability boundary, at which the determinant of the stiffness matrix of the system is zero. At this boundary, it means that the theoretical eigenfrequency of the system would be zero, which is physically impossible. The introduction of the new variable δ, the ratio between the capacitance of the piezoceramic over the negative capacitance, enables the mathematical definition of the boundary, represented by Eq. 3, which is a function of the EMCC (K_{ij}). When tuning the negative capacitance, it is therefore advisable to keep a safety margin from the stability boundary.

$$\delta > \delta_{crit} = K_{ij}^2 - 1 \tag{3}$$

Besides the stability of a theoretical negative capacitance connected to an electromechanical system, the stability of the NIC circuit itself must be taken into account. Since the op-amp is used with both positive

and negative feedback, the circuit is potentially unstable and precaution must be taken. First, a suitable op-amp and the right component values must be chosen, not only to obtain the desired negative capacitance effect, but also to assure stability inside a desired frequency band. Second, the physical construction of the circuit often requires more components than it is shown in Fig. 5, such as a current limit resistor, compensation capacitors, bypass capacitors, etc., which can influence the performance (noise, overheating, etc.) and therefore the stability of the circuit. Finally, for a given piezoceramic displacement, the generated voltage with an RLC-shunt is much higher than with an RL-shunt. The op-amp must hence be able to withstand potentially high voltages and currents, otherwise saturation and non-linear effects will destabilize the circuit. In order to avoid these issues, [12] recently suggested a new NIC circuit design, in which a high voltage op-amp would not be necessary, reducing mass and costs.

Several studies have been carried out using the NIC with shunt damping, but robust circuit design guidelines are yet to be explored. The work developed in [13] uses a closed-loop transfer function analysis to show that the circuit parameters must be chosen in a certain way to obtain stability for the complete electromechanical system. However, precise conditions for all parameters are not derived and the final tuning is still done empirically.

It is important to keep in mind that the mechanical structure, together with the piezoceramic and the shunt circuit, contribute with poles and zeros to form a single control loop. The overall performance and stability depend on each of them, so an understanding of the global system is crucial when designing a smart structure with shunt damping.

5 Optimization Approach

5.1 Host Structure

So as to optimize the smart structure, while maintaining complexity low, two ratios for the sole composite part have been defined for each direction of force input: 1) the maximum normal strain in the direction perpendicular to the polarization of the piezoceramic over the maximum von-Mises strain and 2) the same maximum normal strain over the static stiffness. The first ratio represents how close the composite layup is from an isotropic strain distribution, i.e. how aligned the piezoceramic strain is to the structure's. The second represents how much strain potential there is for a given stiffness. From these two ratios, a third one can be created, taking into account orthogonal directions of force input (in this case, two forces) and also the total mass. The ratios are represented in Eq. 4.

$$\rho_1 = \frac{\max(\varepsilon_{\perp p})}{\max(\varepsilon_{vM})}; \rho_2 = \frac{\max(\varepsilon_{\perp p})}{k_{||p}}; \rho_3 = \frac{1}{m}\prod_{i=X,Y,Z}\rho_1^i\rho_2^i \tag{4}$$

Before optimization takes place, some choices must be made. Carbon fiber was chosen over glass fiber, because it has lower density, higher stiffness and lower price. Unidirectional fiber was preferred rather than woven, so as to better orient strain for a piezoceramic application.

Since mixing continuous and discrete variables can be computationally expensive during the optimization, a layup analysis was first made. More recently, a study has been carried out by [14], where the concept of stacking sequence table is introduced and an evolutionary algorithm optimizes laminated composite structures. In this paper, however, using a simpler approach for the moment, it is assumed that a 90° layer on the external surface can increase the strain under the piezoceramic and eventually enhance the EMCC. A 0° layer on the internal surface increases stiffness of the part. A ±45° layer in between makes a smooth transition and prevents delamination.

Having that in mind, the first step in the optimization flow was carried out, in order to find an initial design. The starting point for the composite beam geometry was chosen to be the same I-beam as the simplified structure, with similar dimensions, but with a hollow profile and a thin wall instead. This represents an additional gain in mass, since material is removed from low strain regions. It is also meant to

ease the manufacturing, in which a prepreg fabric could be used together with a mold and a pressure bag process, for example.

The dimensions of the cross-section were input design variables free to vary. Fixing the layup sequence as 0° / ±45° / 90°, the number of layers for each ply orientation was also defined as an input variable. The objectives of the optimization problem were to fit the desired static stiffness while maximizing ρ_3.

After defining input and output variables, ANSYS Response Surface Optimization Toolbox was used. The FE model is used to calculate a certain number of design points (DP) inside the boundary values for all input variables. The Optimal Space-Filling Design was used to obtain the DP in order to achieve a more uniform space distribution. Afterwards, the response surface is created by interpolating the results from the DP. A neural network algorithm is used to minimize the distance between the interpolation and the DP. This method works well when the number of DP is high. The final objectives of the optimization are obtained using the Multi-Objective Genetic Algorithm.

5.2 Piezoceramic Integration

The next step is to insert the piezoceramic in the FE analysis, so as to carry out a new optimization together with the host structure. In a first approach, however, using an invariable composite structure, a study regarding the piezoceramic size, position and boundary conditions has been done. So as to make the analysis of a smart structure with shunt damping easier, only the DOF corresponding to the Z direction will be further analyzed.

First, the location of the maximum strain level in the structure for the eigenfrequency of interest has been identified. Four rectangular piezoceramics have been hence placed on the outer surface and near the clamp. They are electrically connected in parallel so that only one shunt circuit is used. A sensitivity analysis showed that the thickness of the piezoceramic influences the EMCC more than its width and length, so it has been defined as the input variable at the following steps. Next, two boundary conditions were considered: whether the piezoceramic itself should be clamped or free to move.

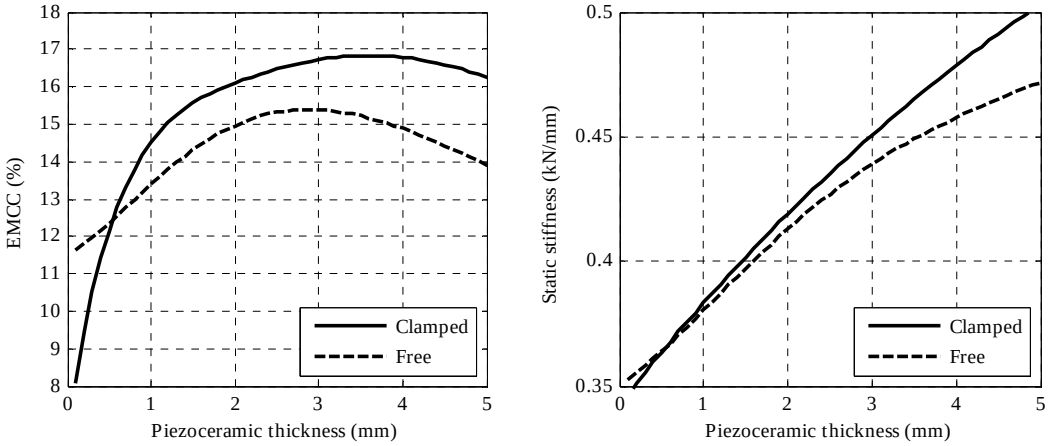

Figure 6: Piezoceramic dimension optimization (left) and its influence on structural behavior (right)

In Fig. 6, it can be seen how the EMCC varies when the thickness of the piezoceramics is changed. For most thickness values, the EMCC shows better values when the piezoceramic is clamped. It can also be noticed that the clamp shifts the optimal thickness to higher values. Nevertheless, since the technical construction of a clamp might not be ideal, in some cases it may not be worth increasing piezoceramic mass and gaining only a little more EMCC. Furthermore, the resultant static stiffness of the composite structure is higher when the piezoceramic is clamped, compared to when it is free.

After analyzing these preliminary statements, the composite structure and the piezoceramics can be now simultaneously optimized. As a starting point, the fitted composite beam was taken together with the

optimal thickness of the piezoceramic obtained previously. The geometries and the number of layers were defined as input variables. The goal of the optimization problem was again to fit the desired static stiffness and maximize ρ_3, but also to maximize the EMCC, since the piezoceramic is now present.

5.3 Equation of Motion

After the optimized FE model is obtained, its most important dynamic parameters are calculated and it is exported as a 1-DOF system. A script is written based on the 1-DOF equation of motion, which describes both electrical and mechanical parts of the system and has been analytically derived in [15]. Considering a forced vibration of a single mass (m), connected to a spring (c_0), a damper (d_0) and also to a piezoceramic, which mechanically behaves as another spring (c_p), the mechanical motion is ruled by Eq. 5.

$$m\ddot{X} + d_0\dot{X} + c_0X + F_p = F \tag{5}$$

Having the eigenfrequency (ω_{mech}) and the static stiffness (c_0) calculated in the FE model, the oscillating mass of the dynamic system is obtained using the classical solution for an undamped 1-DOF system (Eq. 6). The damping coefficient (d_0) comes from the definition of the non-dimensional damping ratio (ζ) in a 1-DOF system where viscous damping is present (Eq. 7).

$$m = m_{dyn} = \frac{c_0}{\omega_{mech}^2} \tag{6}$$

$$d_0 = 2\zeta\sqrt{c_0 m} \tag{7}$$

F_p is the force generated by the piezoceramic, which can be derived from the constitutive electromechanical equations of a linear piezoelectric material. It is defined by Eq. 8,

$$F_p = c_pX - c_pd_pU_p \tag{8}$$

where U_p is the voltage generated by the piezoceramic and d_p is the charge density per unit stress of the electromechanical system, which can be obtained using Eq. 9, as defined in [16].

$$d_p = \frac{1}{c_p}\sqrt{K_{ij}^2 C_{ps}(c_0 + c_p)} \tag{9}$$

Furthermore, the piezoceramic electrically behaves as a voltage generator with an internal capacitance (C_{ps}). From constitutive equations and Kirchhoff's first law, it is possible to obtain the current flowing through the piezoceramic using Eq. 10.

$$I_p = -c_pd_p\dot{X} - C_{ps}\dot{U}_p \tag{10}$$

The piezoceramic is externally connected to a series RLC network, whose equation can be derived using Kirchhoff's second law and the constitutive equations for RLC elements:

$$U_p = L\frac{dI_p}{dt} + RI_p + \frac{1}{C}\int I_p dt \tag{11}$$

Considering the displacement X of the mass, the generated voltage U_p and current I_p as variables, substituting Eq. 8 into Eq. 5 and Eq. 10 into Eq. 11, the dynamic behavior of the system is given by the following equation of motion:

$$\begin{bmatrix} m & 0 & 0 \\ 0 & 0 & 0 \\ 0 & 0 & L \end{bmatrix}\begin{bmatrix} \ddot{X} \\ \ddot{U}_p \\ \ddot{I}_p \end{bmatrix} + \begin{bmatrix} d_0 & 0 & 0 \\ c_pd_p & C_{ps} & 0 \\ 0 & -1 & R \end{bmatrix}\begin{bmatrix} \dot{X} \\ \dot{U}_p \\ \dot{I}_p \end{bmatrix} + \begin{bmatrix} c_0 + c_p & -c_pd_p & 0 \\ 0 & 0 & 1 \\ 0 & 0 & 1/C \end{bmatrix}\begin{bmatrix} X \\ U_p \\ I_p \end{bmatrix} = \begin{bmatrix} F \\ 0 \\ 0 \end{bmatrix} \tag{12}$$

At last, Eq. 12 allows a frequency response function (FRF) calculation of the 1-DOF model and is hence used for all analyses of the shunt damping capabilities.

5.4 Shunt Circuit

Once the piezoceramic integration has been completed and the equation of motion derived, the third step is to integrate the shunt circuit in the exported 1-DOF model. The square of the EMCC can be defined as in Eq. 13, where ω_{open} and ω_{short} are the eigenfrequencies calculated in the FE model when the electrodes of the piezoceramics are open or short circuited, respectively.

$$K_{ij}^2 = \frac{\omega_{open}^2 - \omega_{short}^2}{\omega_{open}^2} \tag{13}$$

In accordance to the optimization method developed in [11] using the frequency response function analysis, the mechanical displacement (X) is minimized when the ratio δ reaches a certain value, defined by Eq. 14. The optimal RLC-shunt parameters are then derived and represented by Eq. 15-17.

$$\delta_{opt} = 2K_{ij}^2 - 1 \tag{14}$$

$$C_{opt} = \frac{C_{ps}}{\delta_{opt}} \tag{15}$$

$$L_{opt} = \frac{1 + \delta_{opt}}{C_{ps}\omega_{open}^2} \tag{16}$$

$$R_{opt} = K_{ij}\sqrt{\frac{2L_{opt}}{C_{ps}}} \tag{17}$$

This method of calculating optimal RLC-shunt parameters relies on calculated values from the FE model, but can be perfectly used with measured values as well. When using measured parameters to fit the FE model, some simulation uncertainties are diminished and the obtained optimal parameters become more reliable. In that sense, [17] recently published another approach to optimize the parameters of a negative capacitance circuit. It uses the concept of strain-induced voltage and minimizes the velocity response of a structure, while assuring stability, based on experimental measurements. However, this method is yet to be validated with a resonant RLC-shunt and especially with a composite structure.

6 Numerical Results and Analyses

The first step in the optimization flow results in the initial composite structure design, as it can be seen in Fig. 7, which is fitted to the simplified metal beam. This composite beam has similar static stiffness and eigenfrequency as the simplified metal beam in both X and Z directions. Moreover, the maximum dynamic strain of the composite beam is higher and the maximum dynamic stress is lower, compared to the simplified structure, since ρ_3 has been maximized.

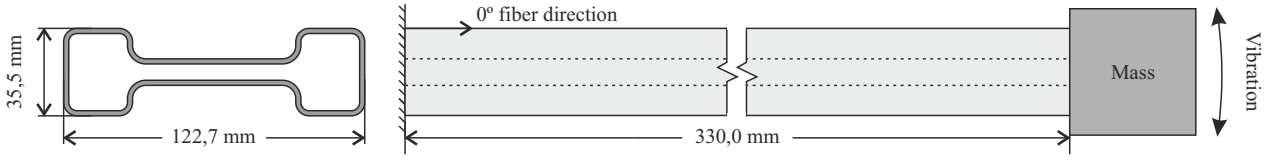

Figure 7: Fitted composite beam

Afterwards, when the composite structure is optimized together with the piezoceramics, a different result is obtained, as it can be seen in Fig. 8.

Table 3 shows a comparison between the three structures obtained so far. It can be noticed that, even though the composite beams have higher cross-section dimensions, due to the hollow profile and material design, they have around one fourth of the mass of the metal beam. More importantly, it can be inferred

from these results that, when optimizing the composite beam together with the piezoceramics, the beam itself is compelled to have a lower stiffness than the specification. However, when the optimal piezoceramic is also taken into account, the calculated stiffness attains the desired value. Moreover, the simultaneous optimization not only fits the target stiffness, but also represents a further gain in mass of the composite and of the piezoceramics, compared to when the sole composite beam is optimized, while still maximizing the EMCC, which is crucial for shunt damping. Even though a high effort to optimize the composite beam was made, the optimal EMCC obtained for the simplified metal beam was higher, which can be explained by a low ρ_1 ratio for the composite designs.

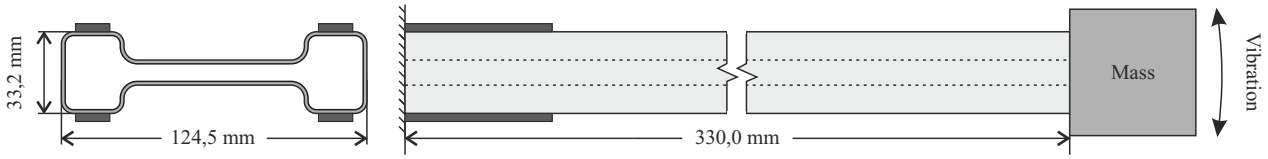

Figure 8: Simultaneously optimized composite beam and piezoceramic transducers

	Property	Simplified metal beam	Fitted composite beam	Optimized composite beam
Passive structure	Outer width (mm)	54,0	122,7	124,5
	Outer height (mm)	19,7	35,5	33,2
	CF layers (mm)	—	15 x 0,23	11 x 0,23
	Beam mass (kg)	2,11	0,58	0,49
	Static stiffness (kN/mm)	0,35	0,34	0,25
	Eigenfrequency (Hz)	59,6	63,2	55,1
Structure + transducers	Optimal piezoceramic dimensions (mm)	14 x 100 x 7,2	14 x 100 x 3,6	14 x 100 x 3,3
	Optimal piezoceramic mass (kg)	0,31	0,16	0,14
	Total mass (kg)	2,42	0,74	0,63
	Static stiffness (kN/mm)	0,65	0,47	0,35
	Eigenfrequency (short circuit, Hz)	72,7	73,7	64,7
	EMCC (%)	18,8	16,5	16,6

Table 3: Steps along the optimization process

Once the 1-DOF parameters of the optimized composite beam are calculated, it is possible to integrate the optimal RLC-shunt circuit into the model. Considering that the piezoceramics have a calculated capacitance of 27,3 nF (C_{ps}), the following optimal values are calculated from Eq. 14-17: δ_{opt} = -0,944, C_{opt} = -28,9 nF, L_{opt} = 11,9 H and R_{opt} = 4,9 kΩ. By using Eq. 12, it is now possible to analyze the impact of the shunt circuit on the dynamic performance of the complete smart structure.

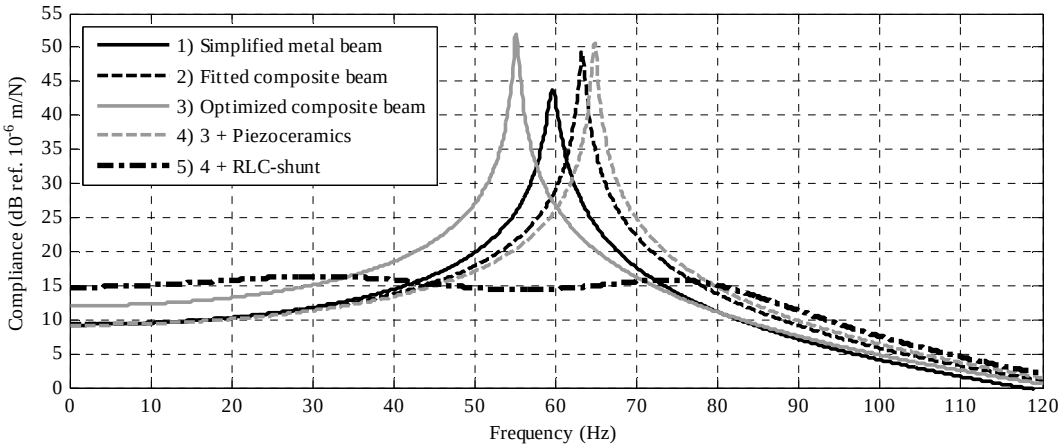

Figure 9: Structural compliances and optimal RLC-shunt FRF

Fig. 9 shows analytical FRFs for several steps along the optimization process. The initial simplified metal beam, which represents the wishbone and defines the target specifications, is plotted in curve 1. When a composite beam is then fitted to have an identical static stiffness, curve 2 is obtained. If a composite beam

is simultaneously optimized with a piezoceramic, in order to fit the target static stiffness, it can be seen that the composite structure alone has been weakened (curve 3) so that when the piezoceramic is computed, the combination behaves with the same static stiffness as the target (curve 4). At last, when the optimal RLC-shunt circuit is connected to the optimized electromechanical system, the system behaves as plotted in curve 5. Even though the optimal RLC-shunt was capable of drastically reducing vibration response (-27 dB compared to the metal beam), it increased the static compliance of the system. This can be another disadvantage of using the NIC, since in order to compensate this effect, more stiffness, and very likely more mass, will have to be brought into the composite structure.

7 Conclusions

To sum up, the global optimization process of a smart structure can be represented in a flowchart diagram, as depicted in Fig. 10. Initially, a composite structure design has been chosen in accordance with a simplified metal structure, that here stands for a real structure, the wishbone. Then, the static and dynamic behavior of the composite beam have been analyzed through FE simulations and optimized to meet the specifications. At this point, it can be stated that a high mass gain is attained. After that, a piezoceramic has been inserted in the design, showing that a mass gain is further possible, while optimizing the EMCC and still meeting specifications. At last, the integration of an optimal RLC-shunt circuit showed that vibration is highly attenuated around the eigenfrequency of the system, but with a cost that its static stiffness is reduced.

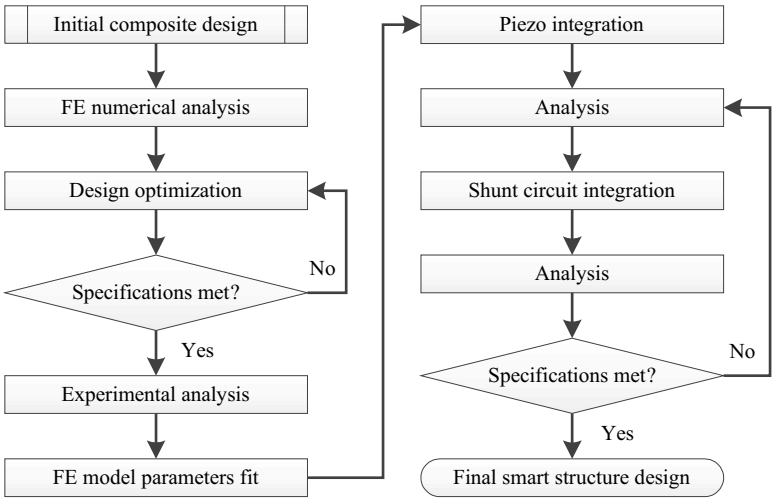

Figure 10: Smart structure optimization flowchart

The next steps of this research will also take into account experimental data during the optimization process, so as to better predict optimized parameters. Another important aspect is to include the static stiffness loss induced by the RLC-shunt circuit, already during the structural optimization, so that the right specification is met in the final design.

Acknowledgements

The research presented in this paper is funded by the German Federal State of Hessen (project “LOEWE Zentrum AdRIA: Adaptronik - Research, Innovation, Application", grant III L 4 - 518/14004(2008)), by the European Commission via the FP7 Marie Curie ITN GRESIMO Project, GA 290050 and via the FP7 ENLIGHT Project, GA 314567. This financial support is gratefully acknowledged.

References

[1] I. Chopra and J. Sirohi, *Smart Structures Theory*, 1st. ed., Cambridge University Press, 2014.

[2] M. I. Frecker, *"Recent advances in optimization of smart structures and actuators,"* Journal of Intelligent Material Systems and Structures, vol. 14, pp. 207-216, 2003.

[3] X. Liu and D. W. Begg, *"On simultaneous optimisation of smart structures – Part I: Theory,"* Computer Methods in Applied Mechanics and Engineering, vol. 184, no. 1, pp. 15-24, 2000.

[4] J. M. S. Moita, V. M. F. Correia, P. G. Martins, C. M. M. Soares and C. A. M. Soares, *"Optimal design in vibration control of adaptive structures using a simulated annealing algorithm,"* Composite Structures, vol. 75, no. 1–4, pp. 79-87, September 2006.

[5] B. Xu, J. P. Ou and J. S. Jiang, *"Integrated optimization of structural topology and control for piezoelectric smart plate based on genetic algorithm,"* Finite Elements in Analysis and Design, vol. 64, pp. 1-12, February 2013.

[6] A. Puck and H. Schürmann, *"Failure analysis of FRP laminates by means of physically based phenomenological models,"* Composites Science and Technology, vol. 58, no. 7, p. 1045–1067, 1998.

[7] Physik Instrumente (PI), *Tutorial on Piezotechnology in Nanopositioning Applications*, 2009.

[8] N. W. Hagood and A. von Flotow, *"Damping of structural vibrations with piezoelectric materials and passive electrical networks,"* Journal of Sound and Vibration, vol. 146, no. 2, pp. 243-268, 22 April 1991.

[9] J. Tang and K. W. Wang, *"Active-passive hybrid piezoelectric networks for vibration control: comparisons and improvement,"* Smart Materials and Structures, pp. 794-806, 2001.

[10] S. Behrens, S. O. R. Moheimani and A. J. Fleming, *"A broadband controller for shunt piezoelectric damping of structural vibration,"* Smart Materials and Structures, vol. 12, p. 18–28, 2003.

[11] M. Neubauer and J. Wallaschek, *"Vibration damping with shunted piezoceramics: Fundamentals and technical applications,"* Mechanical Systems and Signal Processing, vol. 36, no. 1, pp. 36-52, March 2013.

[12] M. Pohl , *"Negative capacitance shunt damping system with optimized characteristics for use with piezoelectric transducers,"* in Proc. SPIE 9057, Active and Passive Smart Structures and Integrated Systems 2014, San Diego, California, USA, March 9, 2014.

[13] S. Manzoni, S. Moschini, M. Redaelli and M. Vanali, *"Vibration attenuation by means of piezoelectric transducer shunted to synthetic negative capacitance,"* Journal of Sound and Vibration, vol. 331, no. 21, pp. 4644-4657, 8 October 2012.

[14] F.-X. Irisarri, A. Lasseigne, F.-H. Leroy and R. Le Riche, *"Optimal design of laminated composite structures with ply drops using stacking sequence tables,"* Composite Structures, vol. 107, pp. 559-569, January 2014.

[15] R. Oleskiewicz, M. Neubauer, T. Krzyzynski and K. Popp, *"Synthetic Impedance Circuits in Semi-Passive Vibration Control with Piezo-Ceramics - Efficiency and Limitations,"* Proceedings in Applied Mathematics and Mechanics, vol. 5, no. 1, pp. 121-122, 2005.

[16] M. Neubauer, R. Oleskiewicz, K. Popp and T. Krzyzynski, *"Optimization of damping and absorbing performance of shunted piezo elements utilizing negative capacitance,"* Journal of Sound and Vibration, vol. 298, no. 1–2, pp. 84-107, 22 November 2006.

[17] B. S. Beck, K. A. Cunefare and M. Collet, *"Response-based tuning of a negative capacitance shunt for vibration control,"* Journal of Intelligent Material Systems and Structures, 7 November 2013 .